

**SAFETY ENGINEERING
ROOT CAUSE REPORT**



9104150170 910409
PDR ADOCK 05000206
P PDR

**SONGS 1 THERMAL SHIELD LOWER
SUPPORT BLOCK FASTENERS
ROOT CAUSE EVALUATION
RCE-91-002
REVISED MARCH 21, 1991**

SONGS 1 THERMAL SHIELD LOWER SUPPORT BLOCK FASTENERS

ROOT CAUSE EVALUATION RCE-91-002

March 21, 1991

Authored By: Mostafa S. Mostafa
Mostafa S. Mostafa

Reviewed By: William W. Strom
William W. Strom

Approved By:

Chong Chiu
C. Chiu, Manager
Safety Engineering

TABLE OF CONTENTS

SONGS 1 THERMAL SHIELD LOWER SUPPORT BLOCK FASTENERS

EXECUTIVE SUMMARY	1
INTRODUCTION	2
EVIDENCE COLLECTION	2
Hidden Bolt H1	3
Hidden Bolt H2	3
Hidden Bolt H3	4
Hidden Bolt H4	4
Short Dowel Pin DS1	5
Short Dowel Pin DS2	5
Long Dowel Pin DL1	5
Long Dowel Pin DL2	6
FAILURE MODE SCENARIOS	7
Dowel Pin Failure Scenario	7
Hidden Bolt Failure Scenario	8
CONCLUSION	9
CORRECTIVE ACTIONS	10

EXECUTIVE SUMMARY

During repairs to the reactor vessel thermal shield in July 1990, the lower support block fasteners were found to be fractured. Figure 3 shows the arrangement of bolts and dowels used to attach the support blocks to the core barrel. Analysis of four segments of the broken hidden bolts indicates they failed due to high stress, low cycle fatigue combined with high stress concentration conditions. Analysis of four segments of the broken dowel pins indicates they failed due to significant fretting wear followed by high stress low cycle fatigue with no stress concentration conditions. In other words, the failure of both the hidden bolts and dowel pins was due to the presence of vibrations with large relative displacements in both axial and radial directions. No evidence of radiation embrittlement was found on any of the examined hidden bolts and dowel pins. The overload zones of the examined fractured hidden bolts and dowel pins exhibited ductile failure.

These large amplitude vibrations were generated when some of the upper flexures broke. Failure of more than one flexure (five out of six failed) caused an imbalance in the support system for the thermal shield. This in turn created uneven loading on the lower support blocks to the point of fatigue crack initiation.

The design of the support block and the type of fasteners enhanced crack initiation and propagation. In particular, the upper portion of the old support block had merely a line of contact with the thermal shield (see Figure 3), this facilitated rocking action between the shield and the block. Also, the old fasteners were threaded all the way to the bolt head. This created a stress riser and generated high stress concentration factors at the base of the head.

The thermal shield repair included a redesign of the upper thermal shield flexures as well as a redesign of the support block and a change in the type of fasteners used. The new support block will provide an area of contact (instead of a very narrow band) between the block and the thermal shield which will minimize the potential rocking action. Bolts with a smooth shank and a large radius of curvature at the head to shank transition and with overall high mechanical properties were used. The upper flexures were redesigned to withstand the calculated stresses.

INTRODUCTION

The reactor vessel thermal shield at SONGS 1, is supported at the bottom by six fixed support blocks on which the bottom of the thermal shield rests. These support blocks are located at 0, 60, 120, 180, 240, and 300 degrees around the perimeter, as illustrated in Figures 1 and 2.

The support blocks are fastened to the core barrel and to the thermal shield by a set of visible bolts and a set of hidden bolts, as illustrated in Figure 3. The original use of the hidden bolts was to facilitate the installation of the thermal shield support blocks onto the core barrel.

Failure of some of the support block bolts had been noted during the Cycle 10 refueling outage. The results of that visual inspection were reported in Westinghouse report #WCAP-12148 dated February 1989 and are summarized in Table 1. In July 1990 SONGS 1 was shut down for Cycle 11 refueling and repair of the thermal shield. The condition of the bolts is summarized in Table 2.

The objective of this report is to determine the fracture mode and the failure mechanism of the support block fasteners, the hidden bolts in particular, and recommend corrective measures.

EVIDENCE COLLECTION

Some of the hidden bolts along with some of the dowel pins were retrieved. Not all of the fasteners could be retrieved for practical reasons. Four broken segments of fractured hidden bolts were found and labeled in this report as H1, H2, H3, and H4. Four broken segments of dowel pins, were retrieved, two of which are segments of short pins labeled as DS1 and DS2. The other two segments are from long dowel pins and were labeled in this report as DL1 and DL2. These fasteners were not identified per location, that is to say, each single fastener cannot be traced back to its specific support block or its location on the block. The support blocks were visually examined during and prior to the removal of the thermal shield.

The retrieved fracture bolts and dowel pins were first photographed in the as found condition and then shipped to General Atomics Laboratory in San Diego, California. There, the fracture surfaces were chemically cleaned from surface oxidation using ultrasonic cleaners and citric acid/water solutions. The cleaned fracture surfaces were then visually examined under a

binocular microscope at magnifications up to 80X and photographs were taken.

No scanning electron microscopy was performed on the fracture surface due to the fact that the surfaces were severely oxidized and rubbed and the fine details of the fracture had been obliterated. Therefore, only macro microscopy was employed in defining the fracture mode.

Hidden Bolt H1

Figures 4 and 5 show two different side views of fractured hidden bolt H1 (0.875" in diameter). Figure 4 illustrates the presence of significant wear on the bolt head at the location marked by the arrow. This indicates that the bolt was in a cocked position in its hole. Figure 6 shows the overall appearance of the fracture face illustrating the presence of multiple fatigue ratchet marks around the perimeter of the fracture which coincides with the thread root. This is further illustrated in Figures 7, 8 and 9. The presence of these ratchet marks is indicative of fatigue fracture under high stress concentration conditions. The macroscopic appearance of the fracture surface indicates a limited fatigue zone estimated to be under 30% of the fracture surface. This in turn is indicative of fracture under relatively high nominal stresses.

Hidden Bolt H2

The appearance of fractured hidden bolt H2 is illustrated in Figures 10 and 11 in the as found condition. The fracture surface in Figure 11 is severely oxidized and the plane of fracture coincides with the first thread root at the bolt head. Figure 12 illustrates significant rubbing damage which is indicative of being fractured for a period of time during which the mating fracture surfaces rubbed against each other.

Figures 13 and 14 illustrate the presence of crack propagation on two planes with initiation at the thread root. This appearance again suggests fatigue fracture under high nominal stresses with high stress concentration conditions. The overload zone appears to cover almost 80% of the fracture surface, marked by a dotted line in Figure 13. In addition, the overall fracture morphology is typical of torsional fatigue conditions.

Hidden Bolt H3

Figures 15 and 16 show two side view photographs of hidden bolt H3 in the as found condition. The plane of fracture appears to coincide with the thread root at the head of the bolt. This was determined by comparing the remaining length of the bolt to its original length.

Figure 16 shows extensive wear and flattening of the sides of the bolt in the vicinity of the fracture and present all around the perimeter of the bolt. This may be indicative of rotational movement in place rather than rocking action. Rocking action would create wear only on one side of the bolt which is not the case here.

Figure 17 shows the appearance of the fracture face in the as found condition illustrating the degree of surface polish and rubbing. This bolt, in comparison with the other retrieved ones, had the maximum rubbing damage. This indicates that this bolt was cracked for a longer period of time than the others.

Figures 18, 19 and 20 show the appearance of the fracture surface of hidden bolt H3 after cleaning. The plane of fracture has a dished nature, similar to the fracture of the hidden bolt H2. The rubbing damage of the fracture surface had significantly erased the details of the fracture, therefore it is difficult to determine the fracture mode of the bolt. However, if one considers the similarity in the overall fracture morphology of this bolt with that of hidden bolts H1, H2 and H4 (which are either convex or concave in nature), it is safe to assume a similar fracture mode. That is, hidden bolt H3 probably failed under similar high stress, low cycle fatigue conditions.

Hidden Bolt H4

The overall appearance of hidden bolt H4 is illustrated in Figure 21. The plane of fracture appears to coincide with the thread root adjacent to the head of the bolt. Figures 22, 23 and 24 show different side views of the fractured end of the bolt in the as found condition. The overall appearance of the fracture face suggest fatigue fracture conditions.

The presence of ratchet marks at the thread root signifies multiple crack initiations as a result of high stress concentration conditions. This is further illustrated in Figures 25, 26, and 27. The overload zone represents nearly 70% of the fracture surface and is typical of torsional loading (see Figure 27). This is indicative of high nominal stress conditions.

Short Dowel Pin DS1

The overall appearance of short dowel pin DS1 is illustrated in Figures 28 and 29. Both figures show the presence of significant wear near the plane of fracture. It is believed that this wear took place prior to the rupture of the pin.

The appearance of the fracture face before and after cleaning is illustrated in Figures 30 and 31 respectively.

A Close-up of the crack initiation zone shown in Figure 32, illustrates the presence of fatigue beach marks and a limited number of ratchet marks. This indicates low stress concentration, but high nominal stresses.

Short Dowel Pin DS2

Figures 33 and 34 show the overall appearance of short dowel pin DS2. Figure 33 illustrates significant fretting wear in the vicinity of the fractured end which is indicative of axial movement in one direction (vibration). The fracture surface was severely oxidized, as shown in Figure 34. The red colored oxide is believed to have occurred during storage after removal.

Figure 35 and 36 show the appearance of the fracture face after cleaning. Evidence of fatigue macroscopic features such as beach marks and thumbnails were evident on the upper portion. The rest of the fracture appears to an overload zone (45° inclined plane). The rubbing damage of the fracture surface indicates that the mating fracture surfaces had remained in contact for a longer period of time than that of DS1. This conclusion is supported by the degree of high temperature oxidation evident on DS2.

Long Dowel Pin DL1

The appearance of long dowel pin DL1 in the as found condition is shown in Figures 37 and 38. Extensive wear is evident in the vicinity of the fractured end. The wear resulted in greater than a 50% reduction of the cross-sectional area. The fracture surface was also heavily oxidized. The red iron oxide appears to have occurred during storage. The fracture surface after cleaning is

illustrated in Figures 39 and 40. The chemical cleaning process resulted in surface pitting in the central portion of the fracture surface as well near the edges as shown in Figure 40.

The overall appearance of the fracture surface indicates the presence of few fatigue thumbnails and beach marks at the outer perimeter of the fracture surface. This is indicative of low stress concentration and relatively high nominal stresses. The overload zone was found to cover most of the fracture surface.

Long Dowel Pin DL2

Figures 41 and 42 show the appearance of the fracture surface of long dowel pin DL2 after cleaning. The fracture surface contains fatigue thumbnail indicating the location of crack initiation (top portion of Figure 42). The reduction in cross-section due to wear was slightly less than that observed in dowel pins DL1, DS1, and DS2.

The overall appearance of the fracture surfaces indicate fatigue fracture and high nominal stresses with low stress concentration conditions.

FAILURE MODE SCENARIOS

The fracture mode scenarios will be confined to the retrieved fasteners (hidden bolts and dowel pins). The failure scenario of the other fasteners will not be addressed in this report since they were not available for the root cause analysis.

The thermal shield flexures were noted to have been broken early in plant life. This transferred uneven loading to the bottom support blocks. The resultant forces were in the axial and radial directions on specific support blocks. The combined loading under normal operating conditions eventually created a significant vibrational condition that led to accelerated rupture of support block bolts and wear in dowel pins.

According to report #WCAP-12148, the hidden bolts were used to facilitate the installation of the lower support blocks, and were not designed to carry any significant loading. The other fasteners including the long upper bolts, the lower bolts, and the dowel pins were placed to carry the specified design loading. The upper bolts and the lower bolts were placed to restrain any relative radial displacements, while the dowel pins were placed to restrain any relative axial displacements. If any of these fasteners were to break or to significantly wear, significant loading would be transferred to the hidden bolts in both axial and radial directions.

Dowel Pin Failure Scenario

Fracture analysis of the dowel pins indicated significant uneven wear near the fractured end. This is indicative of axial vibration in one direction that caused the dowel pins to fret unevenly. The wear caused a significant reduction in the pin cross-section which produced an increase in the magnitude of the applied stresses and may have created bending conditions. This in turn initiated fatigue cracks that propagated under high stresses, low cycle conditions. This conclusion is supported by the fact that the fatigue zone covers a small fraction of the fracture surface.

Hidden Bolt Failure Scenario

During the cycle 10 refueling outage in 1989, three out of eighteen visible bolts on the support blocks were reported to be broken. This condition combined with evidence of fretting wear of the dowel pins leads to the suggestion that axial displacement (wear on the pins) and radial displacement (broken long bolts) occurred.

The remaining bolts including the hidden bolts would then be exposed to heavy vibrational conditions in both axial and radial directions. This, coupled with the fact that the hidden bolts had a high stress concentration condition, resulted in fatigue cracks initiated all around the perimeter at the first thread root in most cases. These cracks then propagated under high stress conditions to the point of failure. This scenario is supported by the fact that three out of the four hidden bolts evaluated had crack initiation at the first thread root below the bolt head. The fatigue zone was found to cover only a small surface area fraction while the rest was an overload zone.

The fact that the overload zone reflected torsional overloading morphology can be explained by the vibrational displacements in the axial and radial directions which created a thread loosening and translational movement of the bolt. If the bolt was pinned at one end, the other end would experience a twisting action, i.e. torsional stress conditions. Also, problems with hole alignment for the new support block bolts were observed during the repair of the thermal shield. Skewed bolt holes would have added to the twisting action of the hidden bolt near the head.

In summary, it is believed that rupture or severe damage of the long bolts combined with wear in the dowel pins preceded the rupture of the hidden bolts. This is supported by the fact that at each support block, where a hidden bolt was broken, the long bolts were broken as well as the dowel pins with one exception at 180° support block. The hidden bolt was broken and no report of failures to the long bolt nor to the dowel pins, see Table 2.

Since the hidden bolt at 180° was not identified during removal, and only four segments were retrieved and analyzed for fracture mode determination, it is difficult to predict the root cause of failure of this hidden bolt. However, since most of the bolt holes were aligned, but skewed through the block/core barrel, and there was no record of the applied torque during initial installation, it is possible that this bolt experienced stress conditions different than that experienced by other hidden bolts as a result of initial installation.

According to the initial blue prints of the support block fasteners, all bolts should have a smooth shank below the bolt head, see Figure 3.d. The retrieved four hidden bolts were threaded to the head and did not conform to the original drawings.

CONCLUSION

Fracture analysis of the retrieved hidden bolts indicated the fracture mode to be high nominal stress, low cycle fatigue with high stress concentration conditions.

Fracture analysis of the dowel pins indicated fretting wear followed by low cycle, high stress fatigue conditions. Each of the examined hidden bolts and dowel pins had fractured in a ductile fashion and no evidence of brittle fracture was found.

The failure of the examined lower support block fasteners was due to the vibration of the support block relative to thermal shield and core barrel. This vibration was created by the fracture of thermal shield upper flexures. This was enhanced by the type of the fastener and its geometry as well as the support block configuration.

The recommended corrective actions in this report are in agreement with Westinghouse report WCAP-12148. However, Westinghouse predicted the hidden bolts would fail from overloading conditions. This analysis shows the hidden bolts failed from high stress, low cycle fatigue conditions.

CORRECTIVE ACTIONS

The fracture analysis of the retrieved support blocks hidden bolts and dowel pins indicated that the failure mode was high stress, low cycle fatigue. The hidden bolts also had high stress concentration. This situation was created as a result of vibration of the support block with large relative displacement in the axial and radial directions.

The bolt design was changed to reduce the stress concentration factor. The new bolts have flat smooth shanks with a large radius of curvature at the head to shank transition region.

A design change was made to the support blocks to provide an area contact instead of a line contact between the block and thermal shield. This reduces the potential for rocking action, thereby reducing potential vibration significantly.

A design change was made to the dowel pins to assure tight fitting of the dowel pins in their slots, thereby reducing any potential of fretting wear. This was accomplished by increasing the diameter of dowel pin and by changing the installation procedure to allow for shrink fitting.

A design change of the thermal shield flexures was also made to assure they will withstand operating stresses. The details of this design change are beyond the scope of this report.

FIGURE 1. Schematic of the Thermal Shield Support System

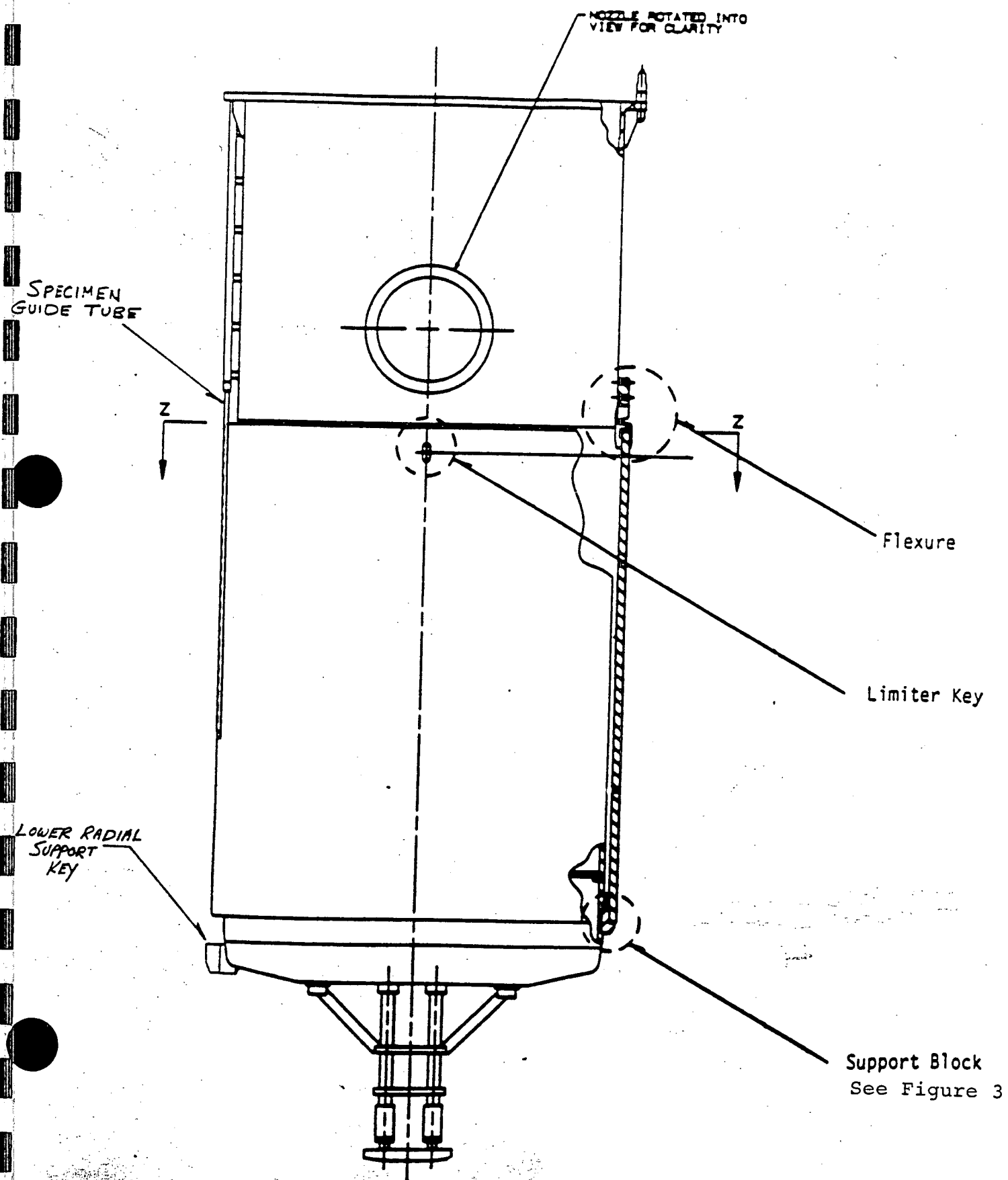


FIGURE 2. Plain View of the Thermal Shield Support System

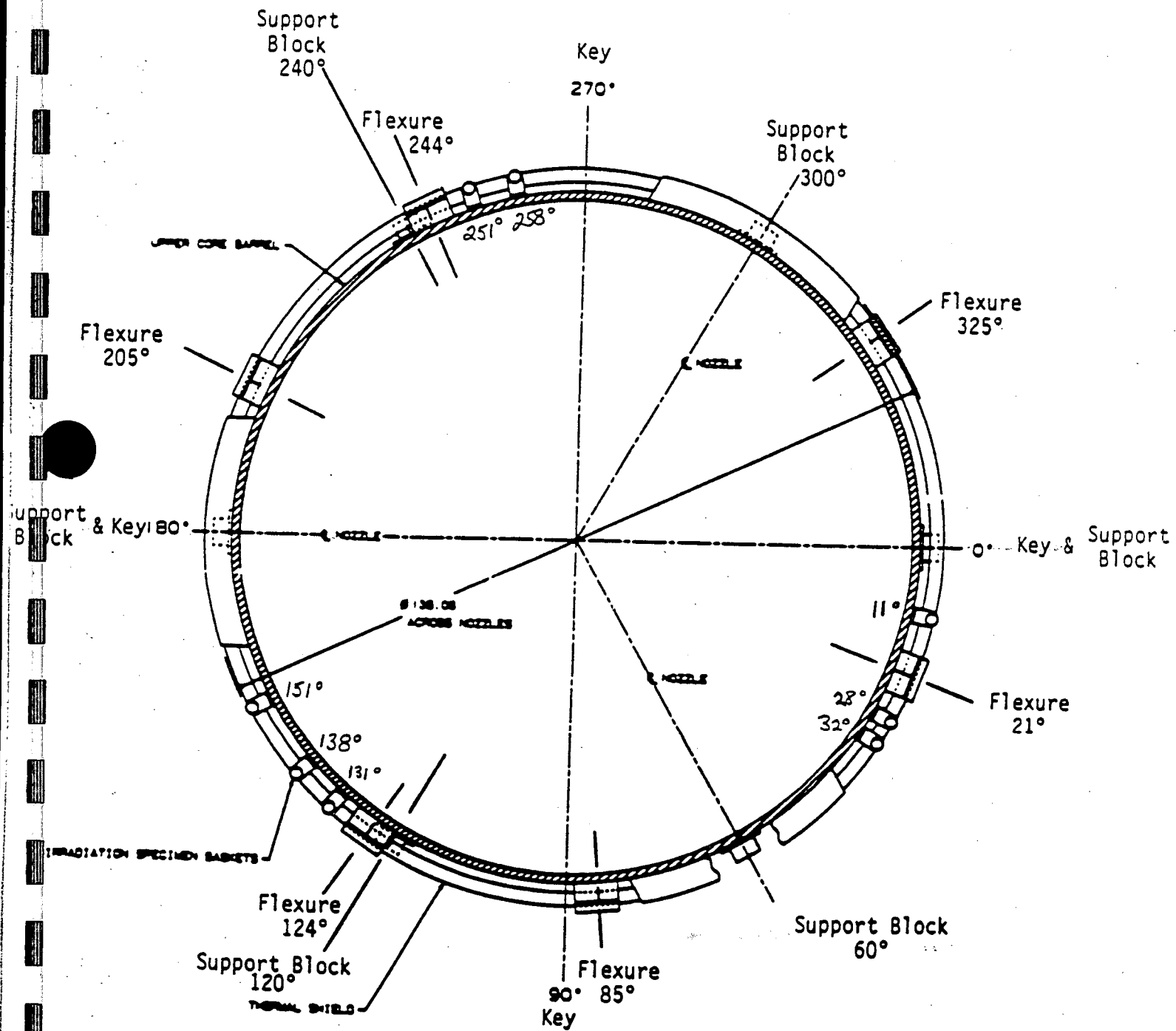


FIGURE 3a. Original Support Block Design

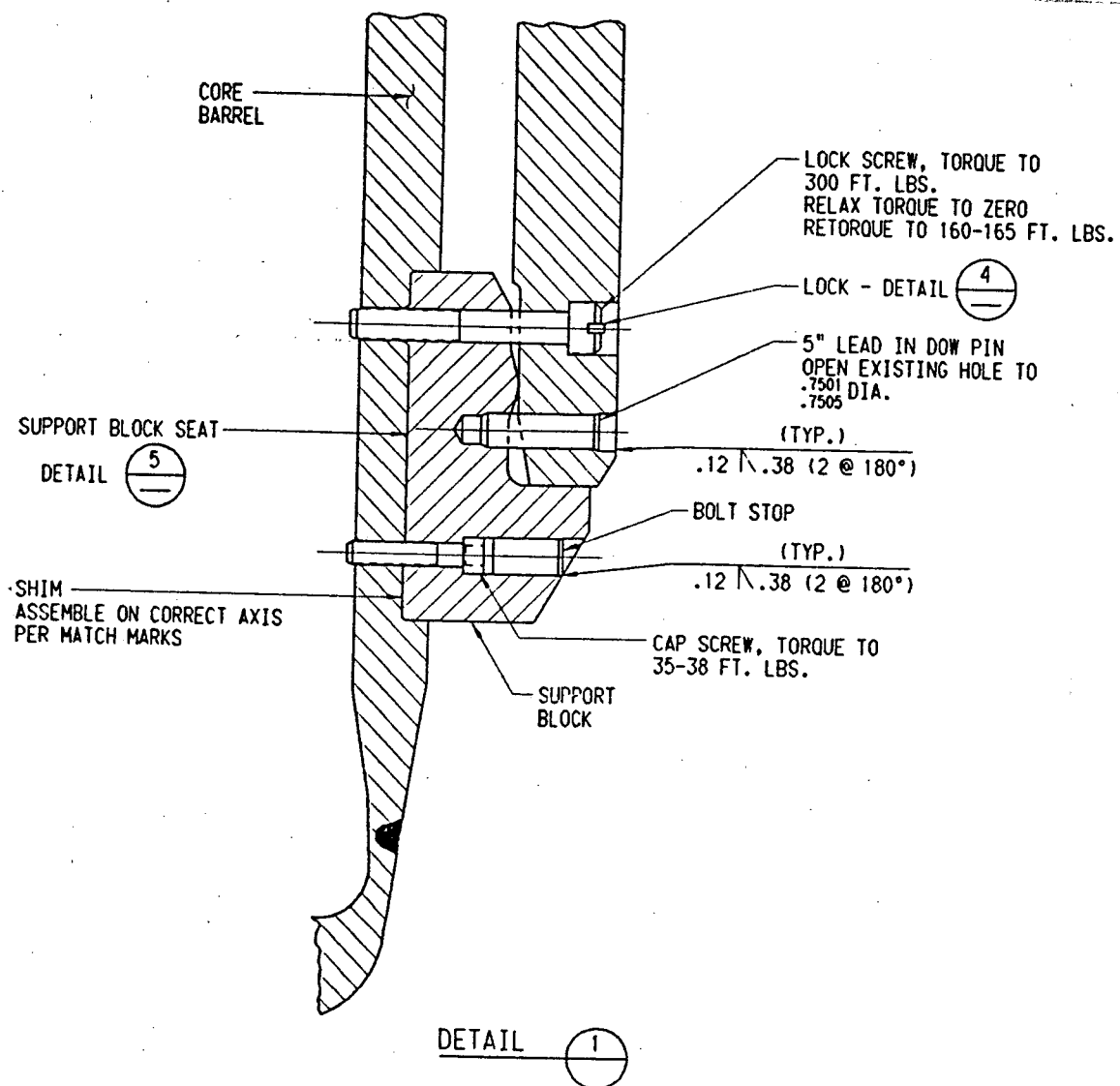
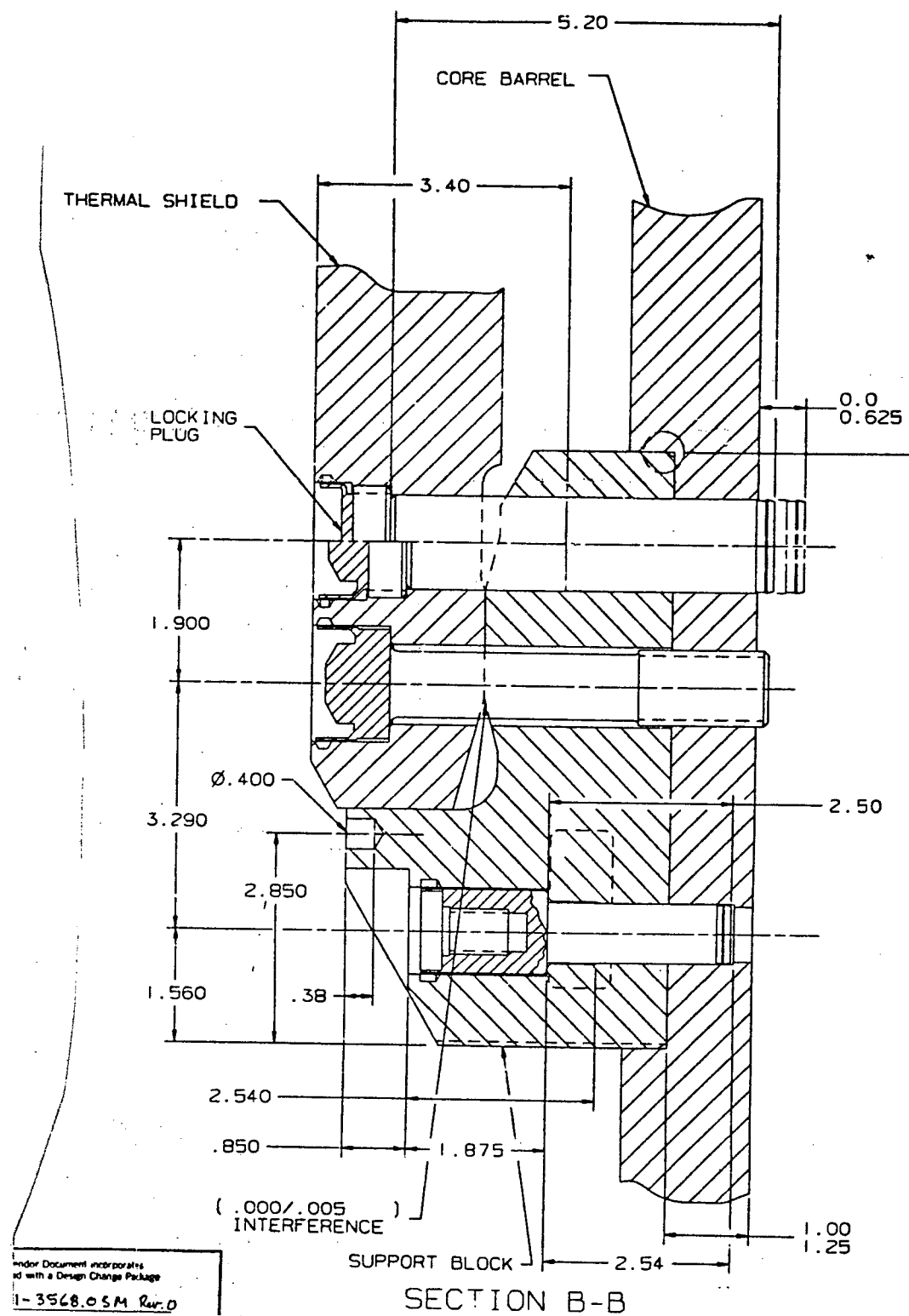


FIGURE 3b. Replacement Support Block Design



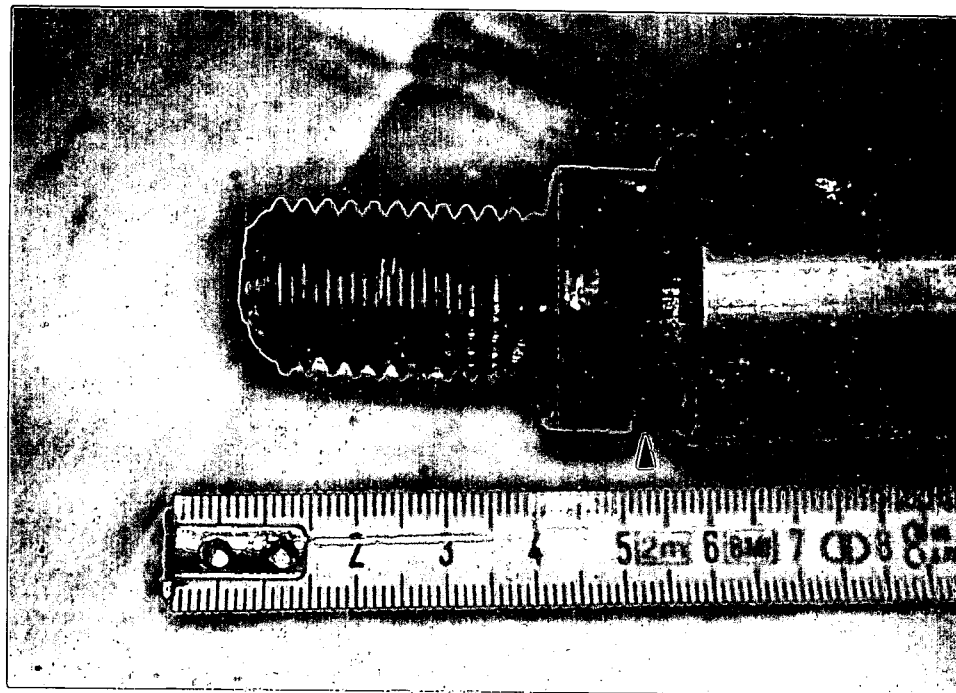


FIGURE 4. Appearance of hidden bolt H1 as found. The arrow points to significant uneven wear on the bolt head.

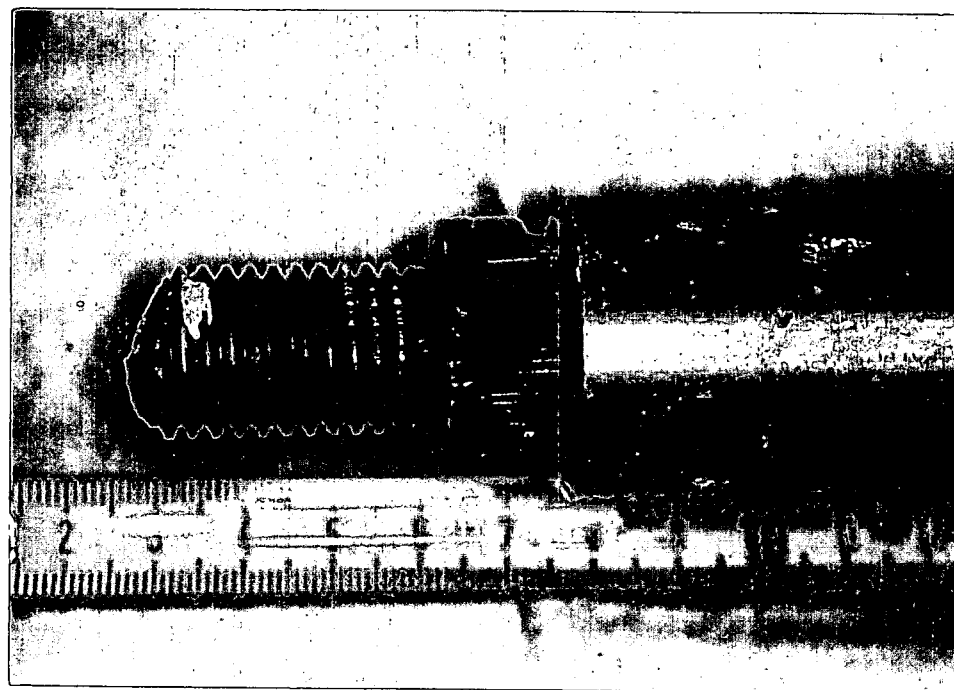


FIGURE 5. Another view of hidden bolt H1.

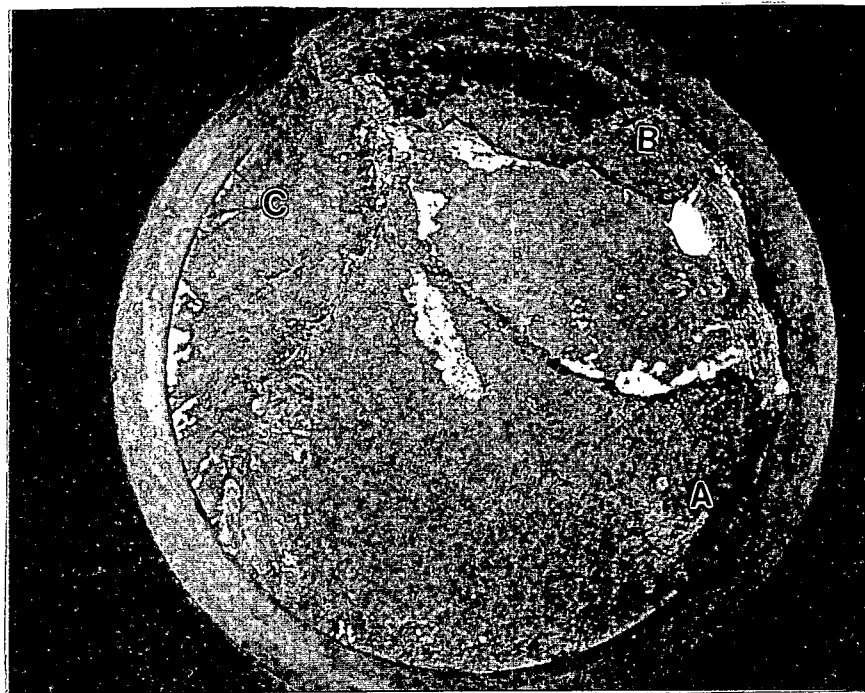


FIGURE 6. Macro photograph of the fracture face of hidden bolt H1 after cleaning. 5x

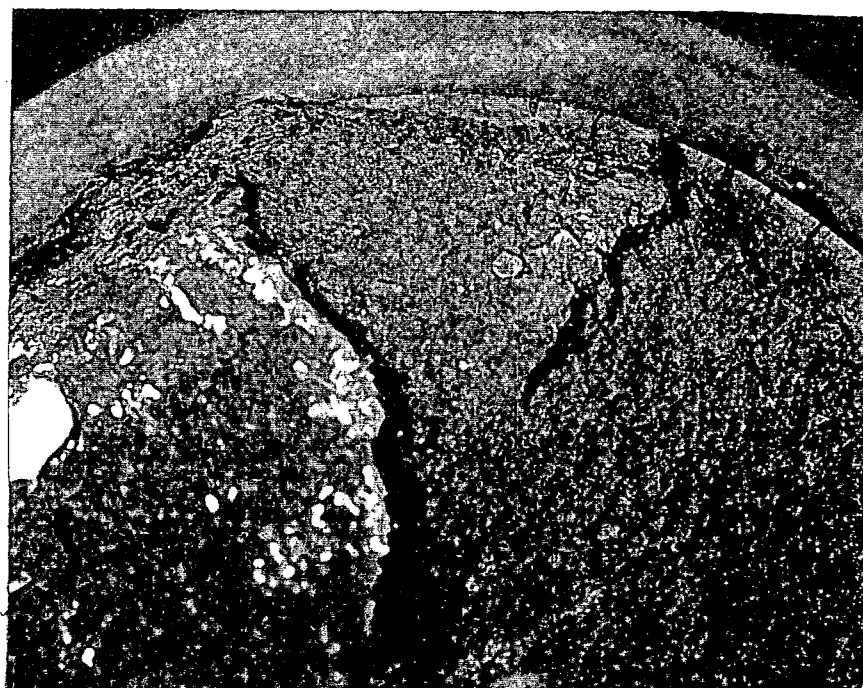


FIGURE 7. Close-up view of Area "A", Figure 6, showing fatigue ratchet marks at the thread root. 10x

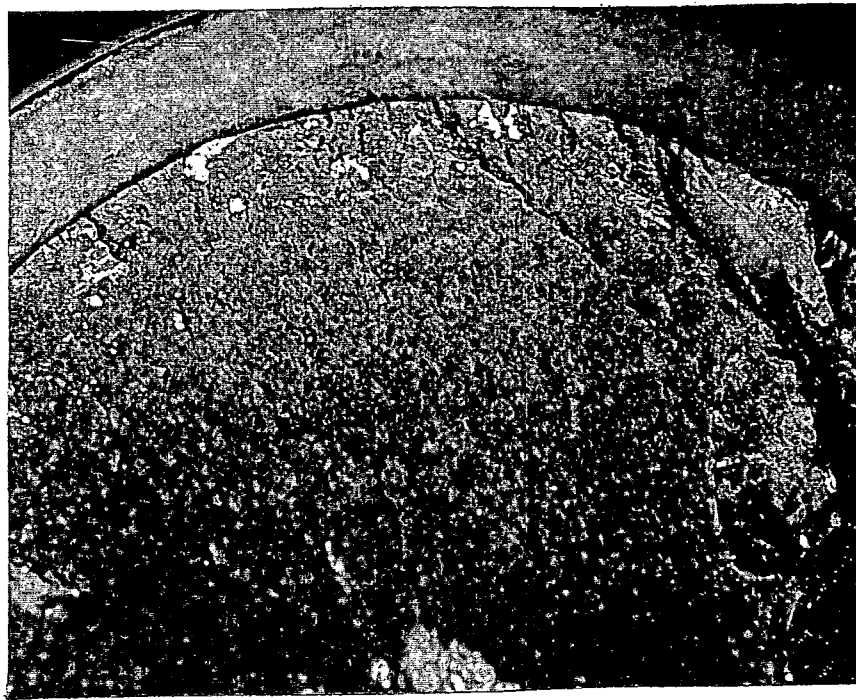


FIGURE 8. Close-up view of Area "B", Figure 6, showing fatigue ratchet marks at the thread root. 10x

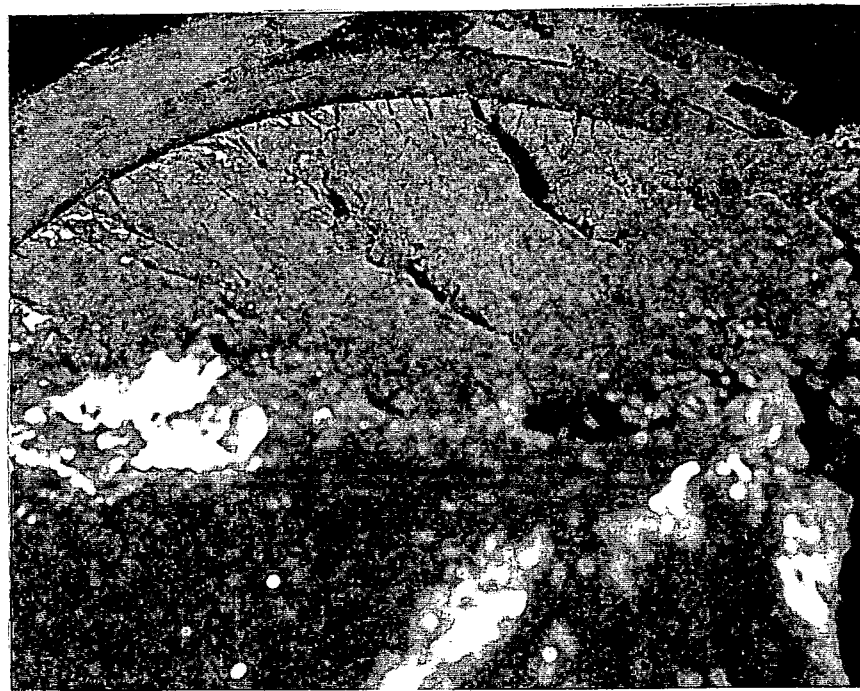


FIGURE 9. Close-up view of Area "C", Figure 6, showing fatigue ratchet marks. 10x

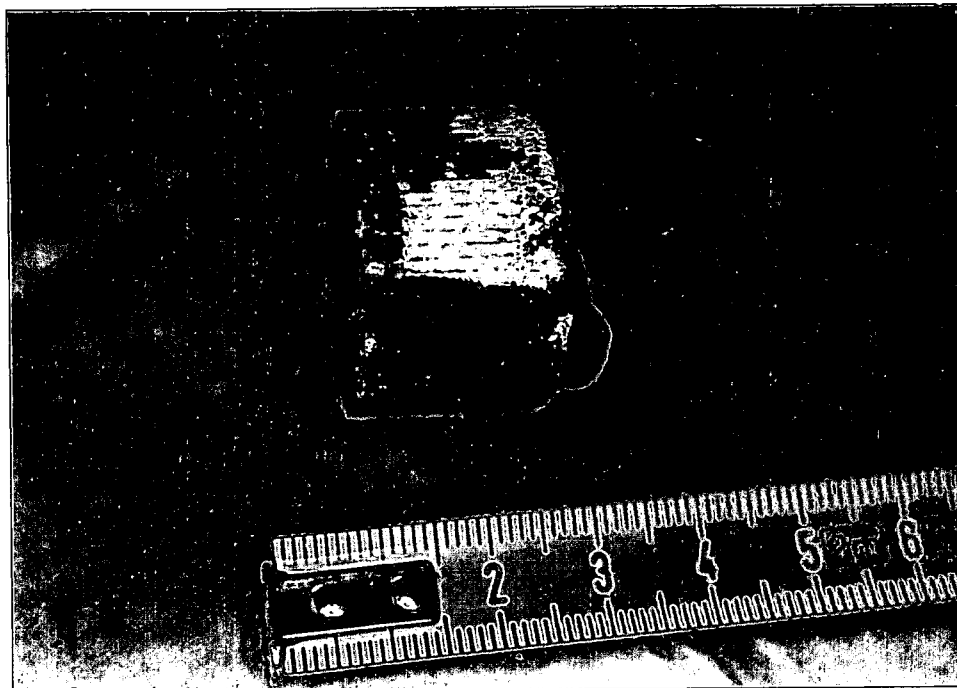


FIGURE 10. Appearance of hidden bolt H2, as found condition.



FIGURE 11. Appearance of the fracture face of hidden bolt H2 illustrating severe high temperature oxidation.

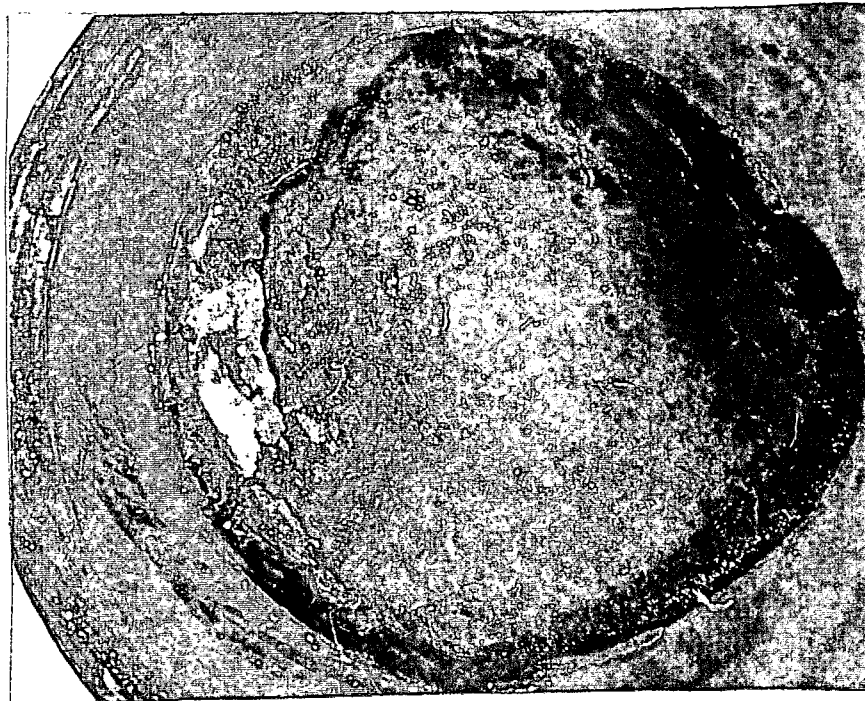


FIGURE 12. Appearance of the fracture face of hidden bolt H2 after cleaning, illustrating severe rubbing damage. 4.5x

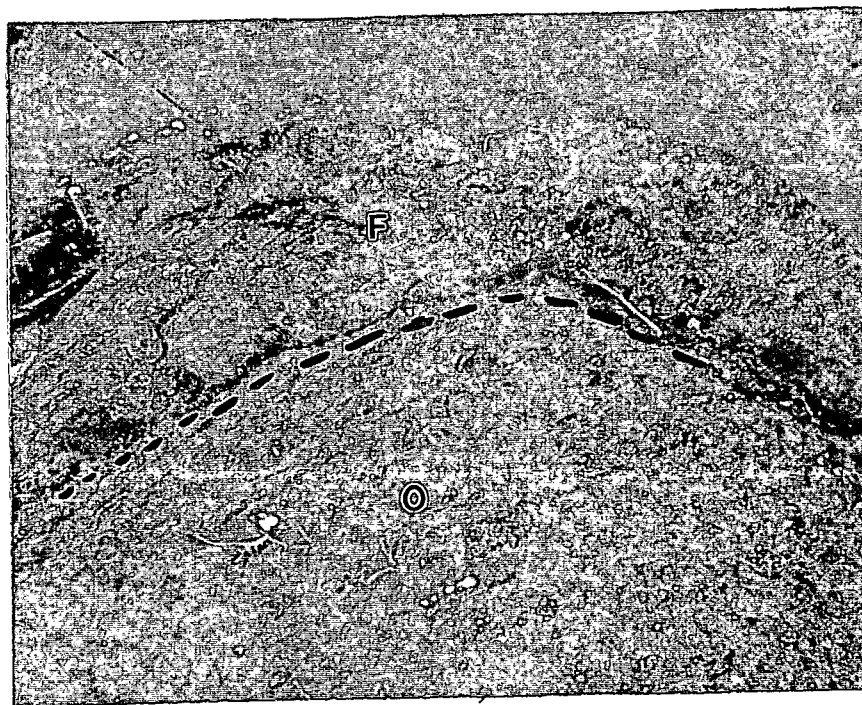


FIGURE 13. Close-up view of the fracture face of hidden bolt H2 showing torsional overload at "O" and possible fatigue zone "F" that had been obliterated by rubbing. 10x

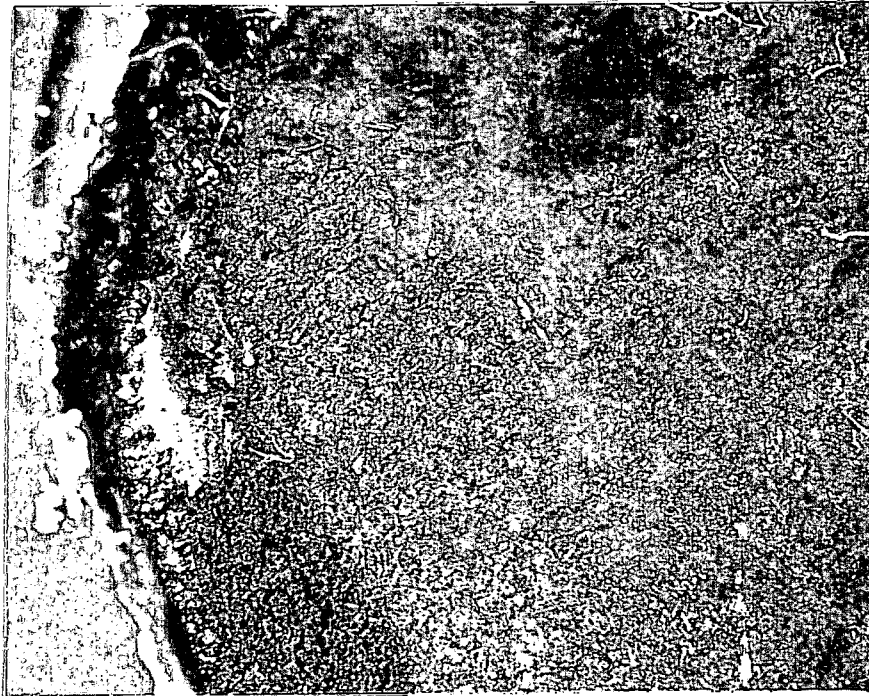


FIGURE 14. Another close-up view of hidden bolt H2. 10x

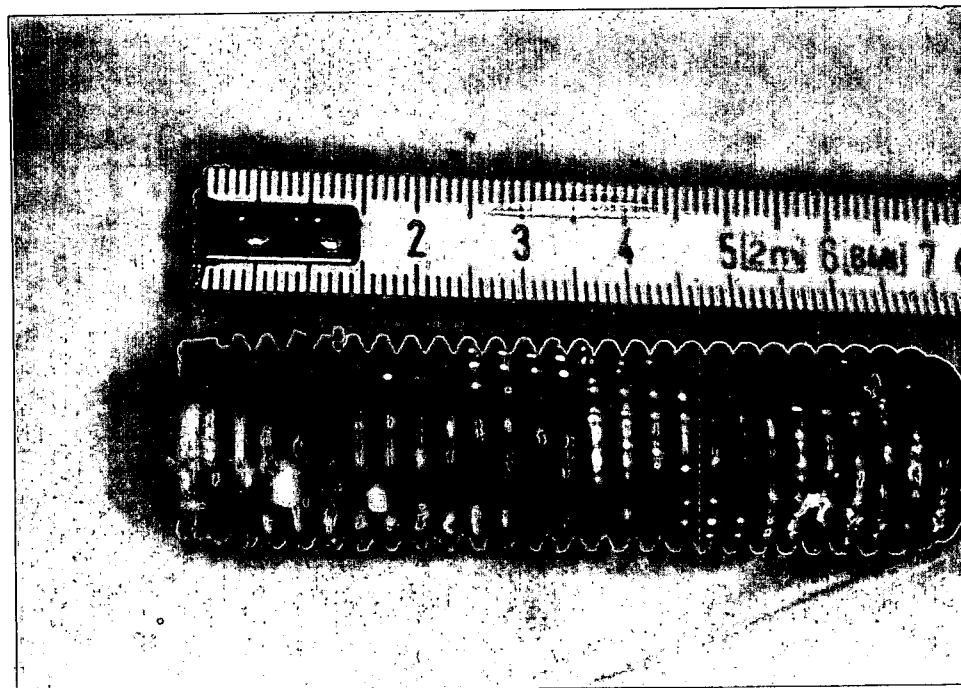


FIGURE 15. Appearance of hidden bolt H3, as found.

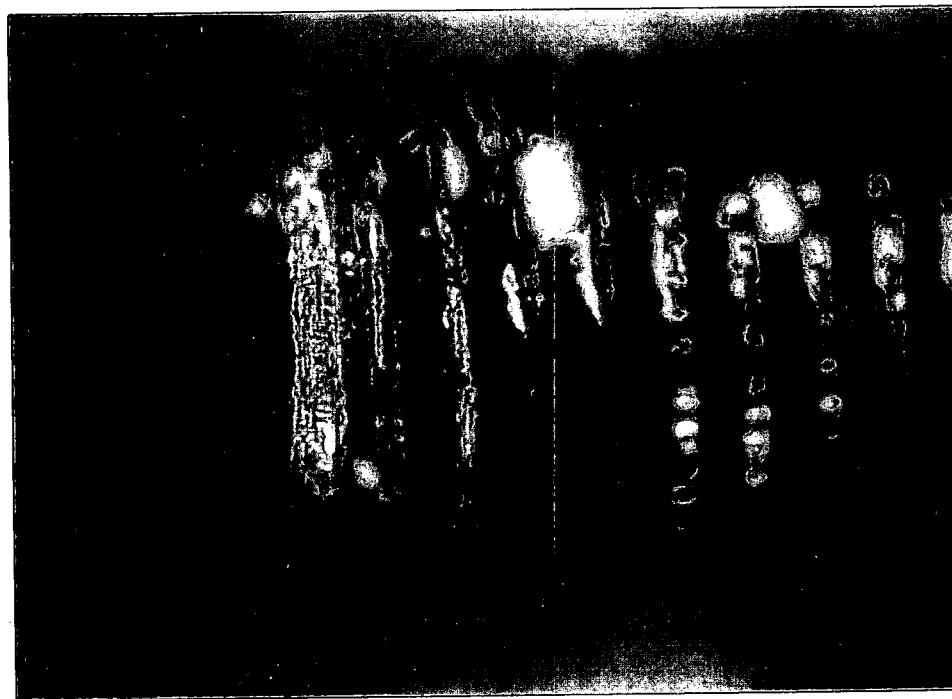


FIGURE 16. Close-up side view of the fractured end of hidden bolt H3, illustrating the presence of uneven side wear, as found condition.

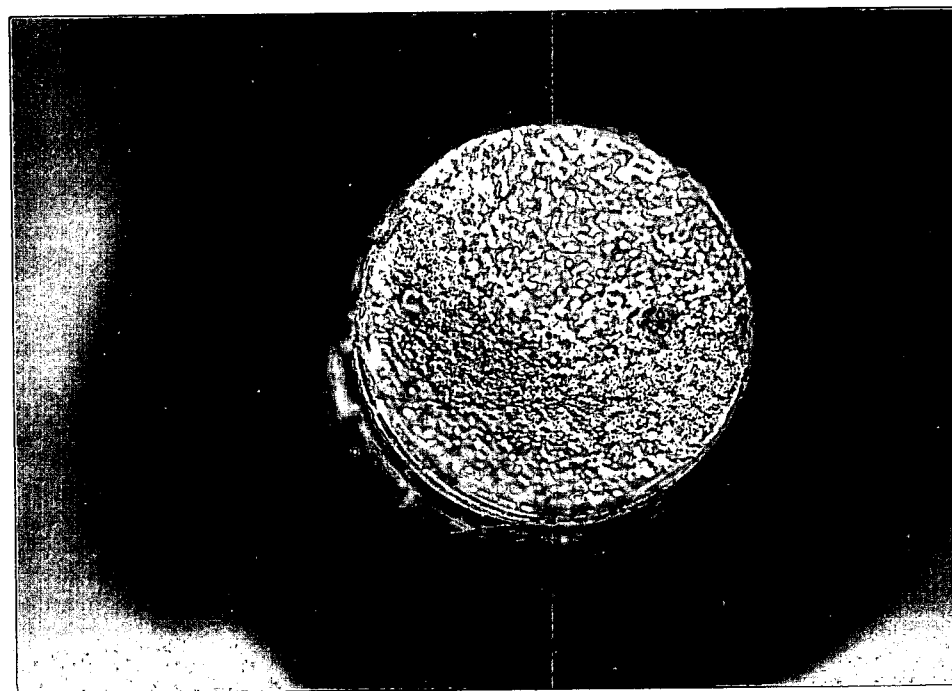


FIGURE 17. Appearance of the fracture face of hidden bolt H3 illustrating significant rubbing damage.

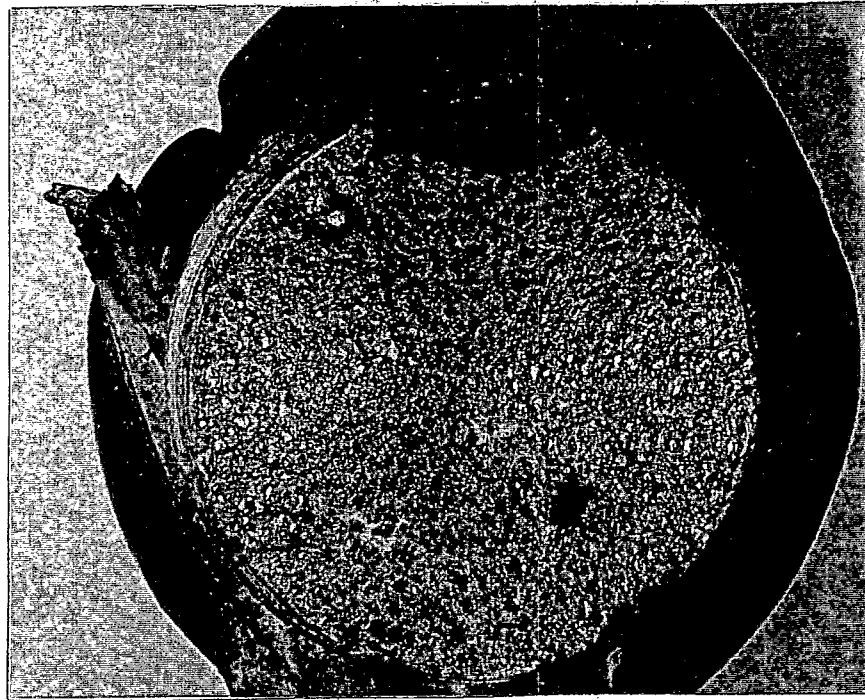


FIGURE 18. Appearance of the fracture face of hidden bolt H3 after cleaning, illustrating significant rubbing damage. 4x

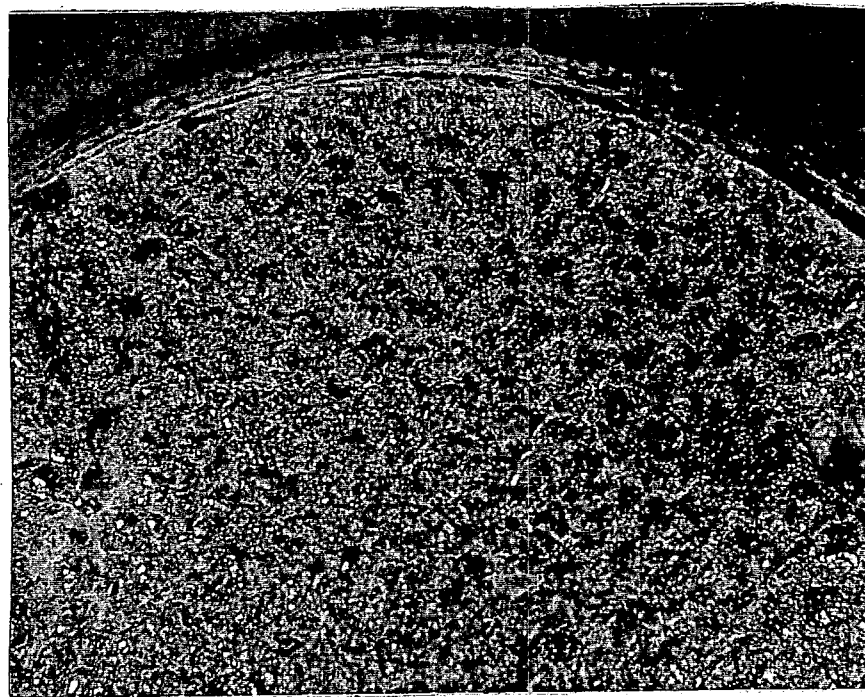


FIGURE 19. Close-up view of Figure 18. 10x

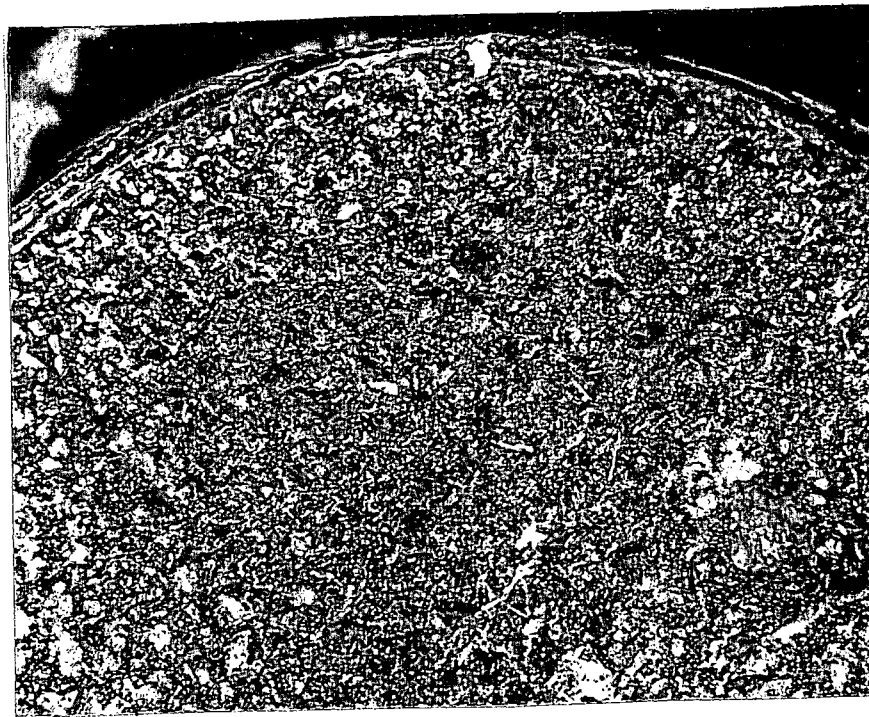


FIGURE 20. Close-up view of Figure 18. 10x

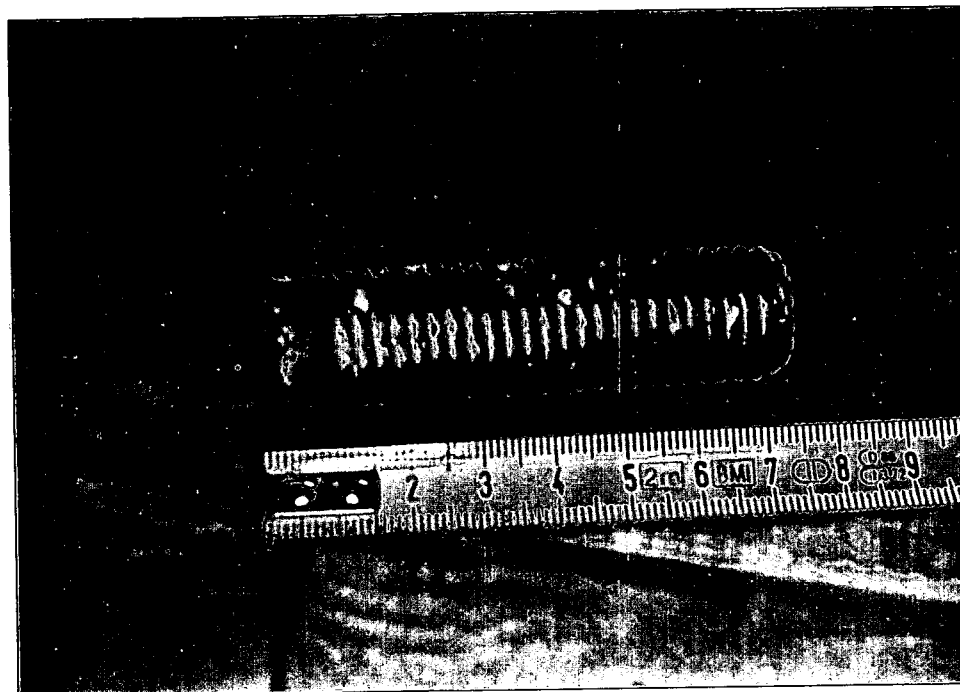


FIGURE 21. Appearance of hidden bolt H4, as found condition.

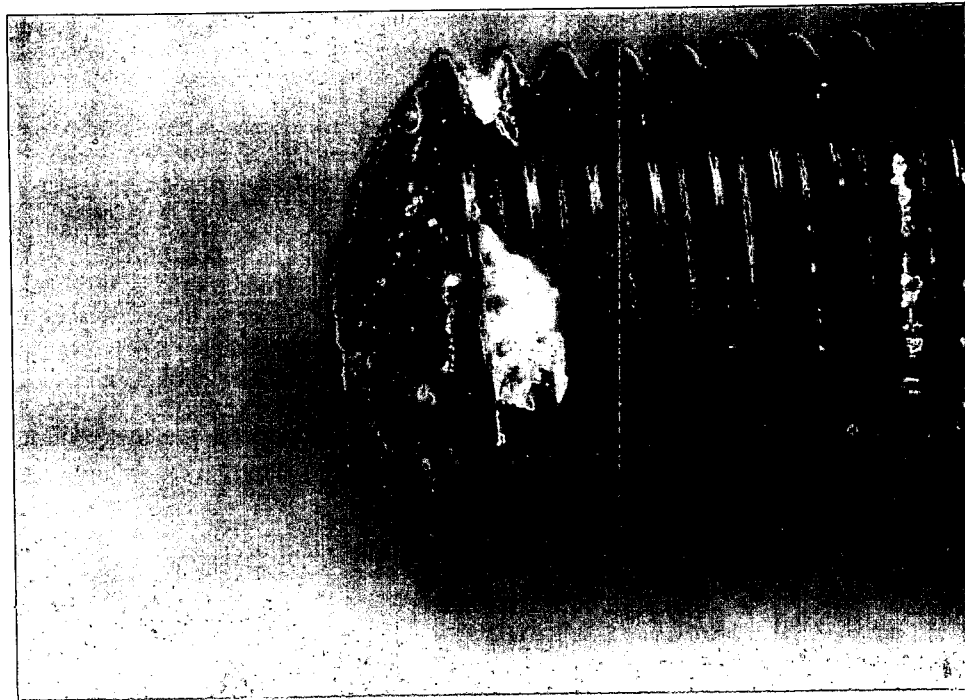


FIGURE 22. Close-up side view of hidden bolt H4, as found condition.

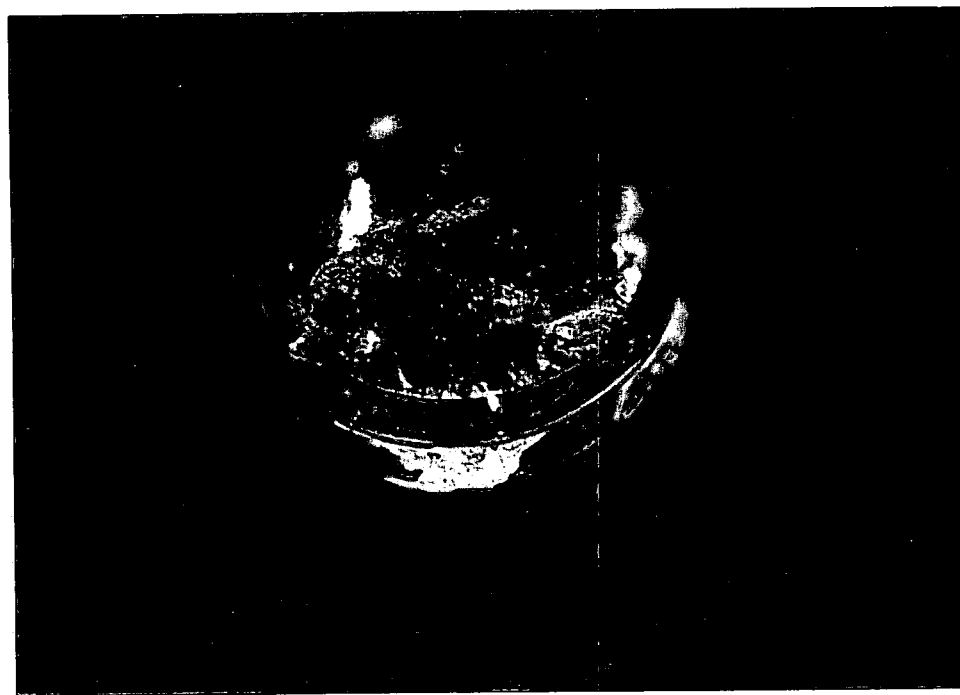


FIGURE 23. Close-up view of the fracture face of hidden bolt H4, as found condition.

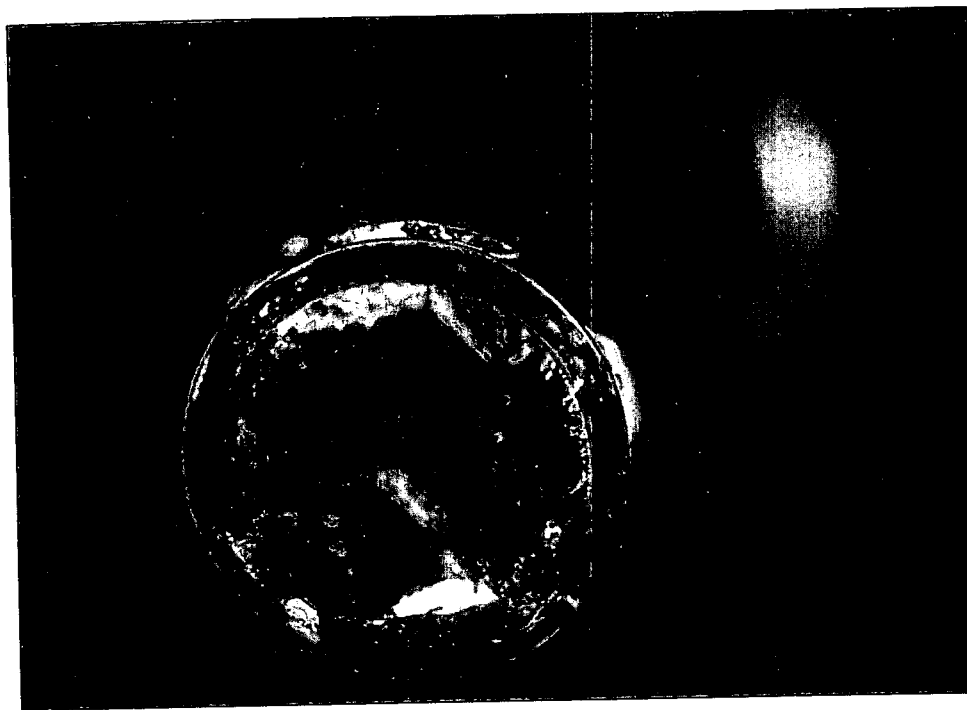


FIGURE 24. Another close-up view of the fracture face of hidden bolt H4, as found condition.

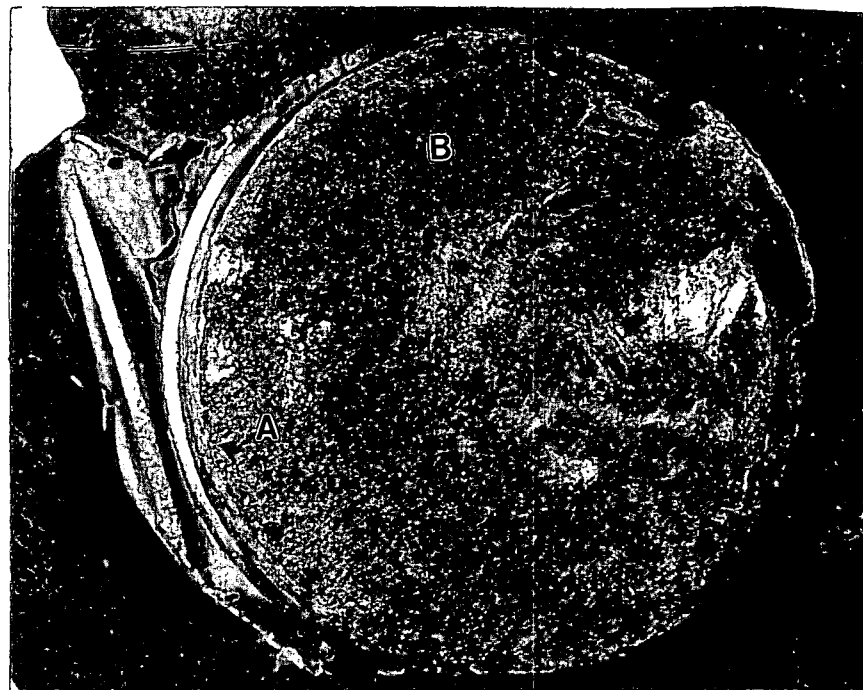


FIGURE 25. Appearance of the fracture face of hidden bolt H4 after cleaning. Area "A" represents fatigue crack initiation. 4.5x

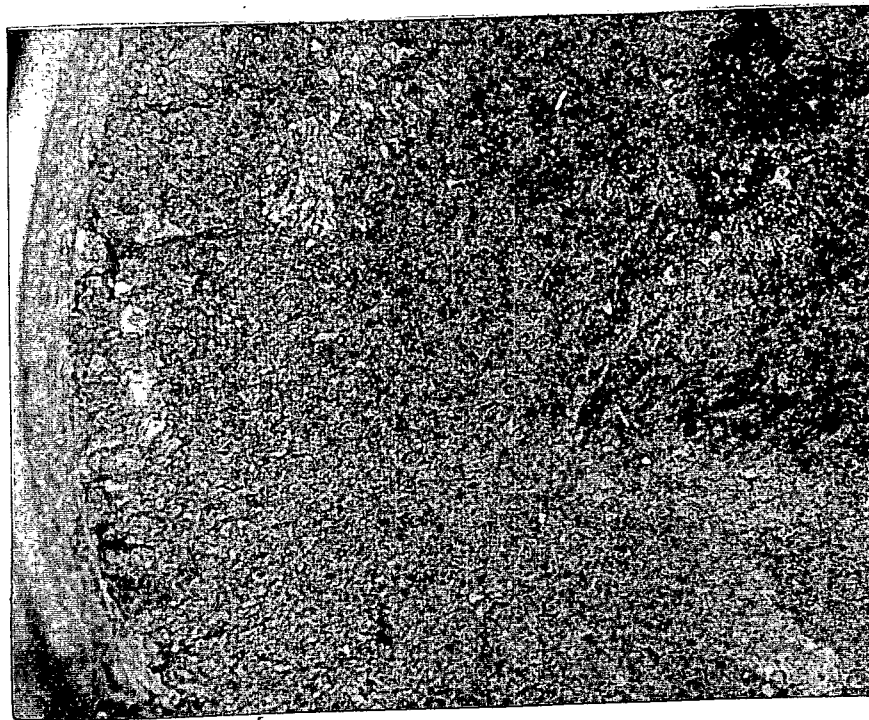


FIGURE 26. Close-up view of Area "A", Figure 25, showing fatigue ratchet marks. 10x



FIGURE 27. Close-up view of Area "B", Figure 25, illustrating torsional type of overloading fracture. 10x

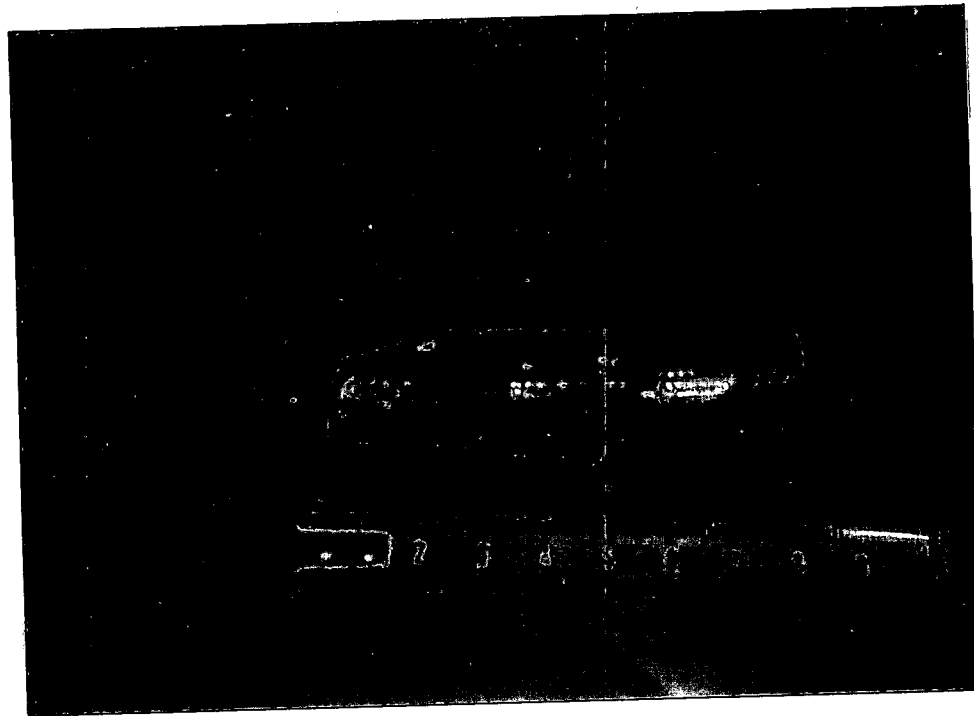


FIGURE 28. Appearance of the short dowel pin DS1, as found condition.

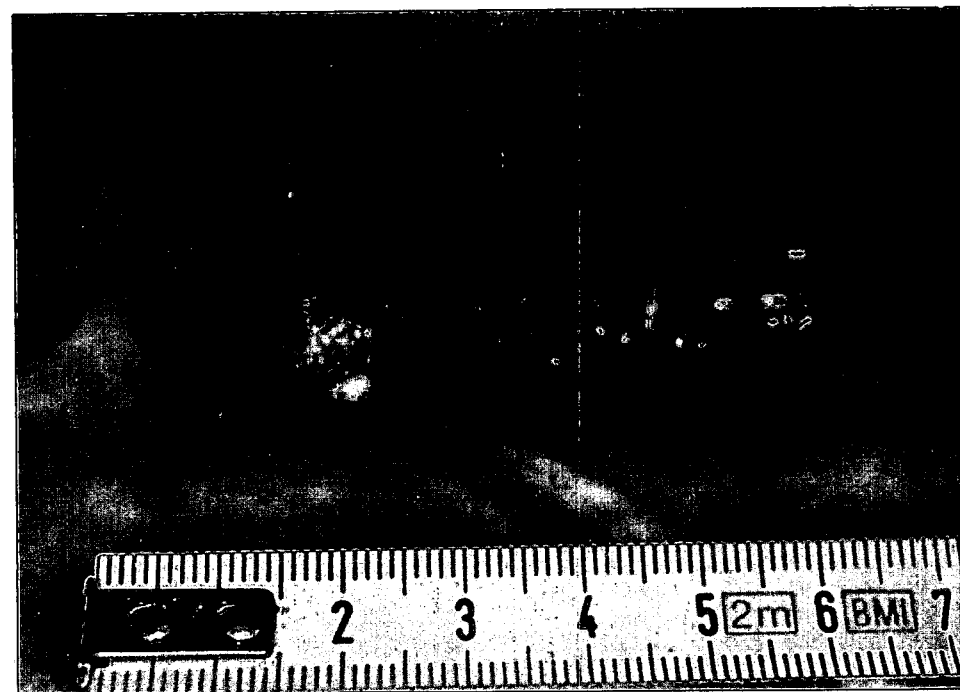


FIGURE 29. Close-up view of the fractured end of short dowel pin DS1, illustrating non-uniform wear.

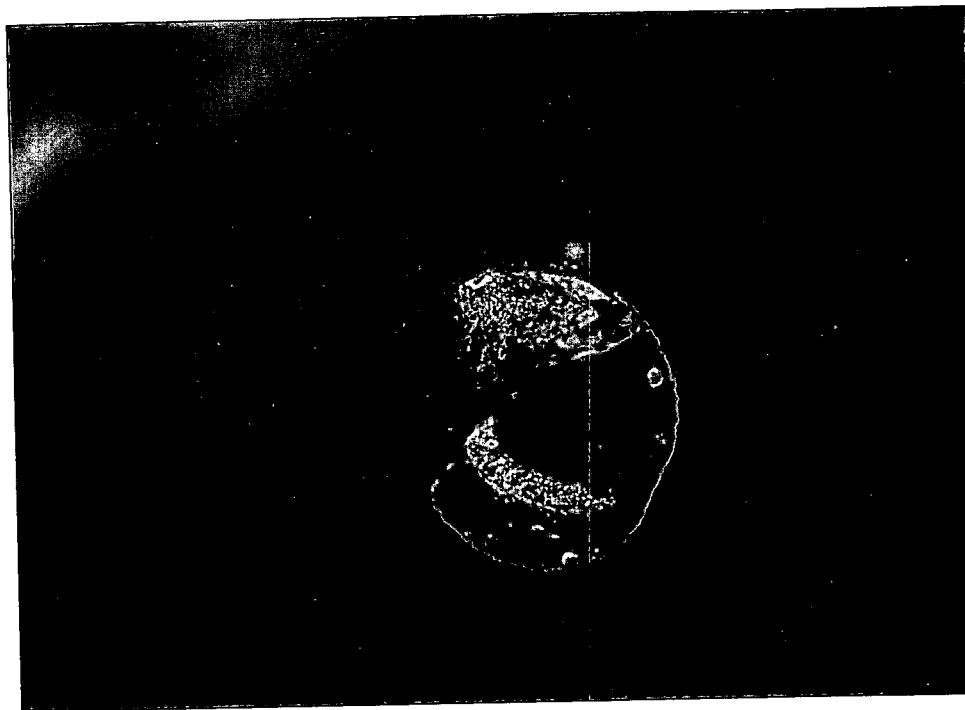


FIGURE 30. Appearance of the fracture face of short dowel pin DS1, as found condition.



FIGURE 31. Close-up view of the fracture face of short dowel pin DS1 after cleaning. 5x



FIGURE 32. Close-up view of Figure 31, illustrating what appears to be beach marks from fatigue followed by an overload zone on an inclined plane. 10x

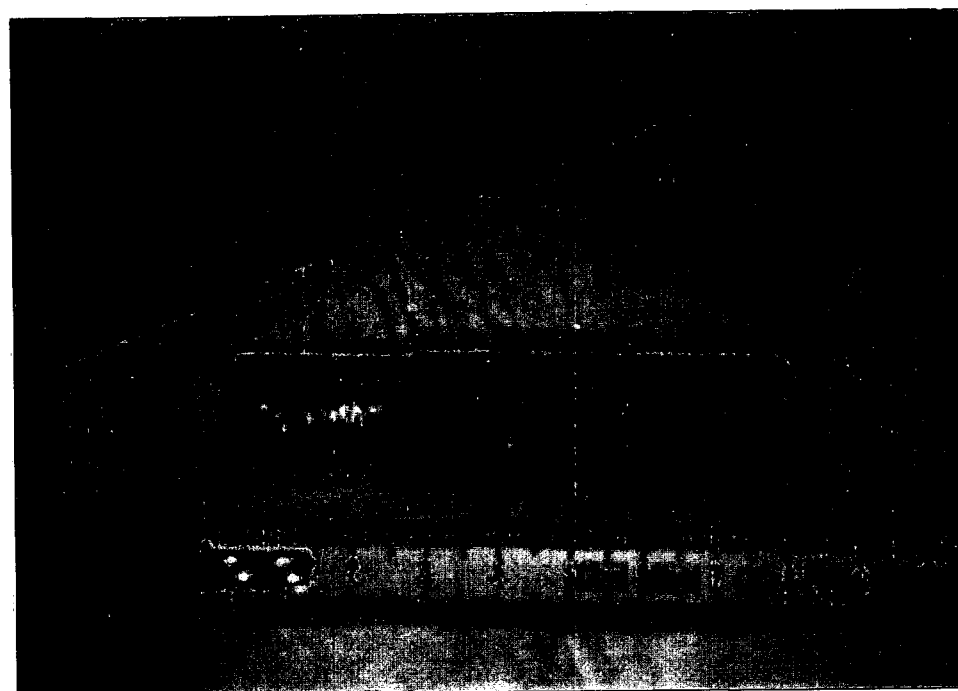


FIGURE 33. Appearance of short dowel pin DS2, as found condition, illustrating uneven wear.

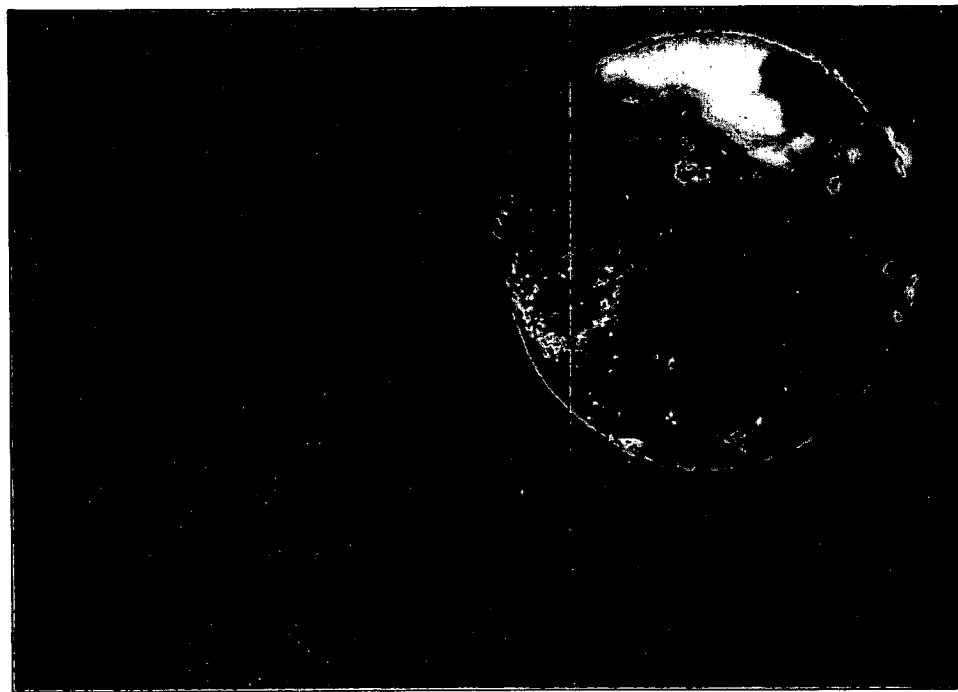


FIGURE 34. Appearance of the fracture face of short dowel pin DS2, as found condition.

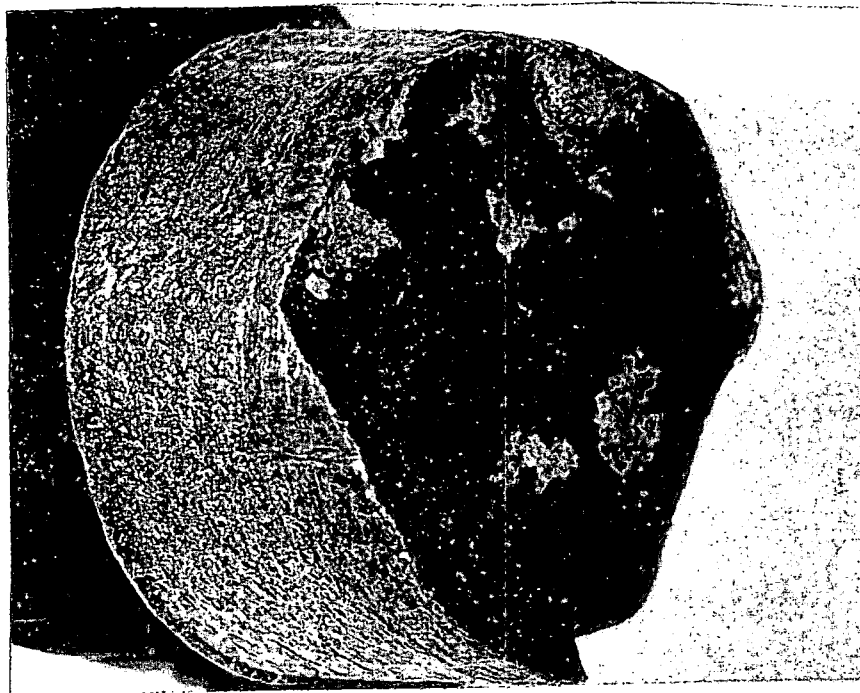


FIGURE 35. Appearance of the fracture face of short dowel pin DS2 after cleaning, illustrating fatigue thumbnails and beach marks followed by an overload fracture on an inclined plane at approximately 45°. 5x.



FIGURE 36. Another view of the fracture surface of short dowel pin DS2 after cleaning. 5x.

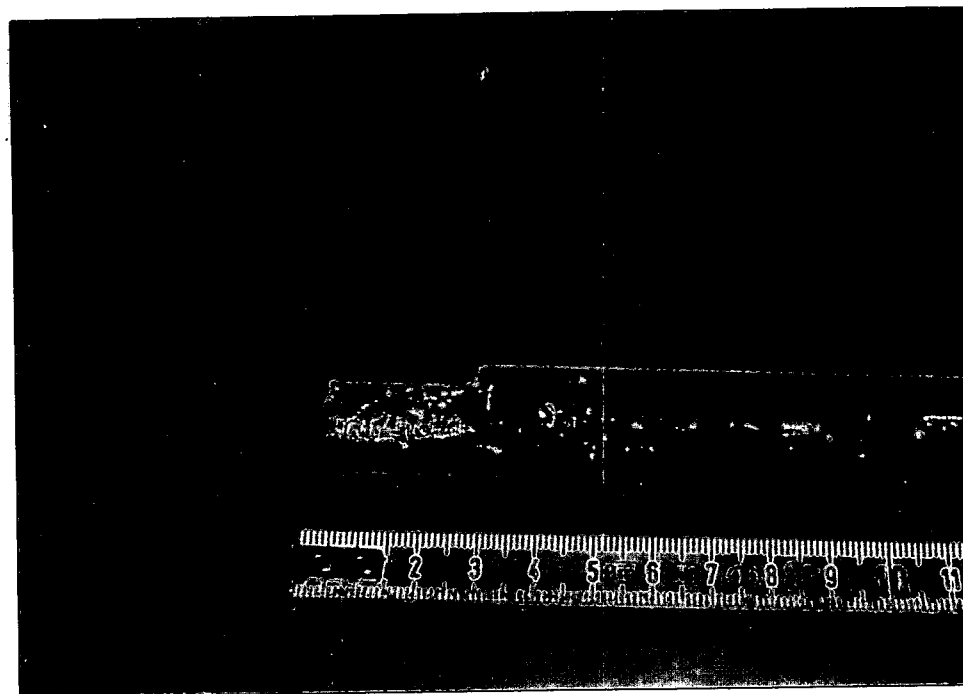


FIGURE 37. Appearance of long dowel pin DL1 showing significant uneven wear, as found condition.

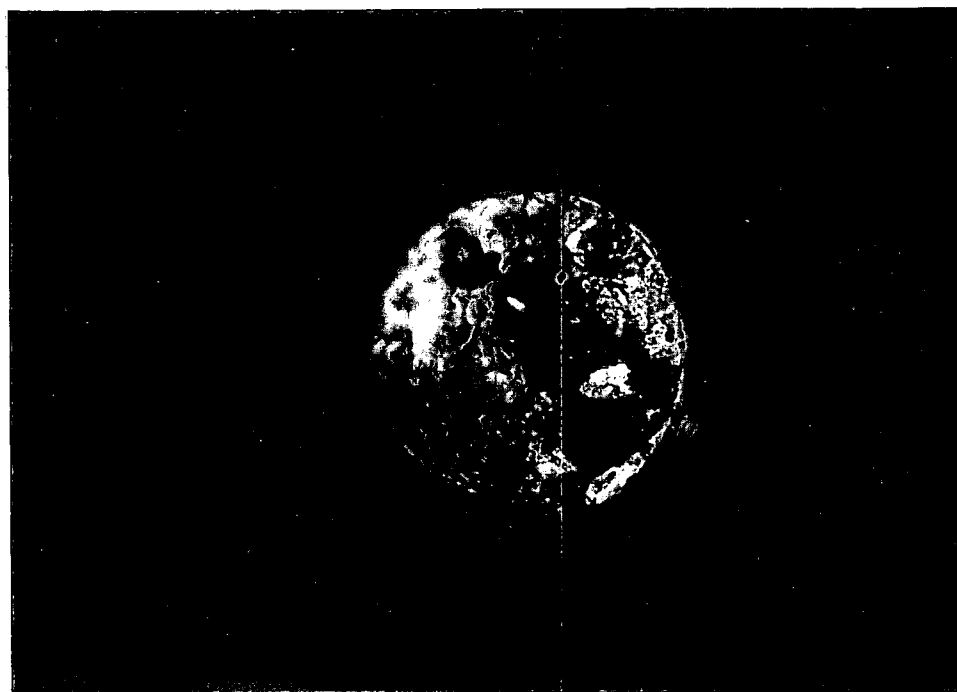


FIGURE 38. Appearance of the fracture face of long dowel pin DL1, as found condition.

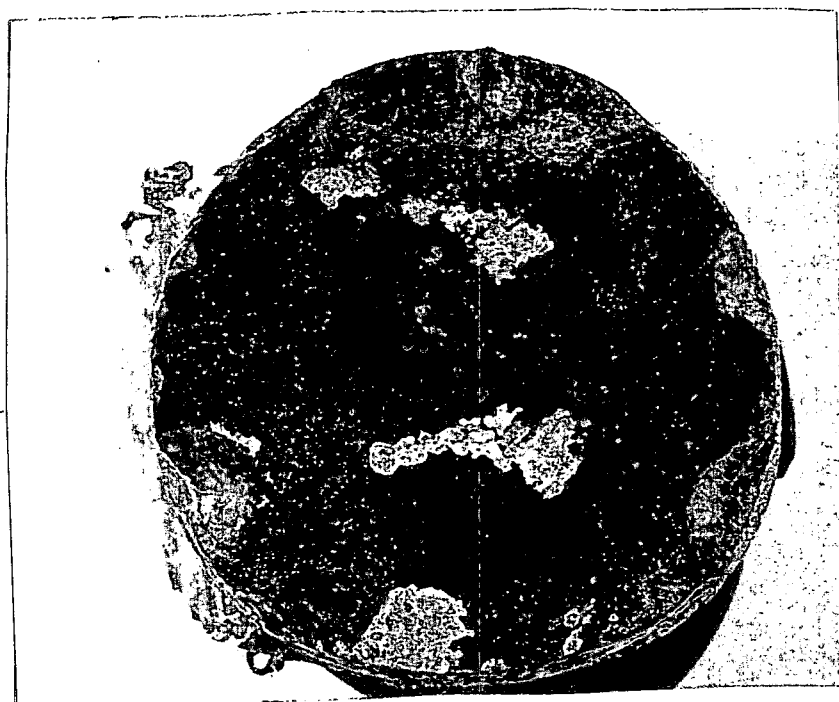


FIGURE 39. Appearance of fracture face of long dowel pin DL1 after cleaning, illustrating the presence of multiple fatigue thumbnails and beach marks. 4.5x

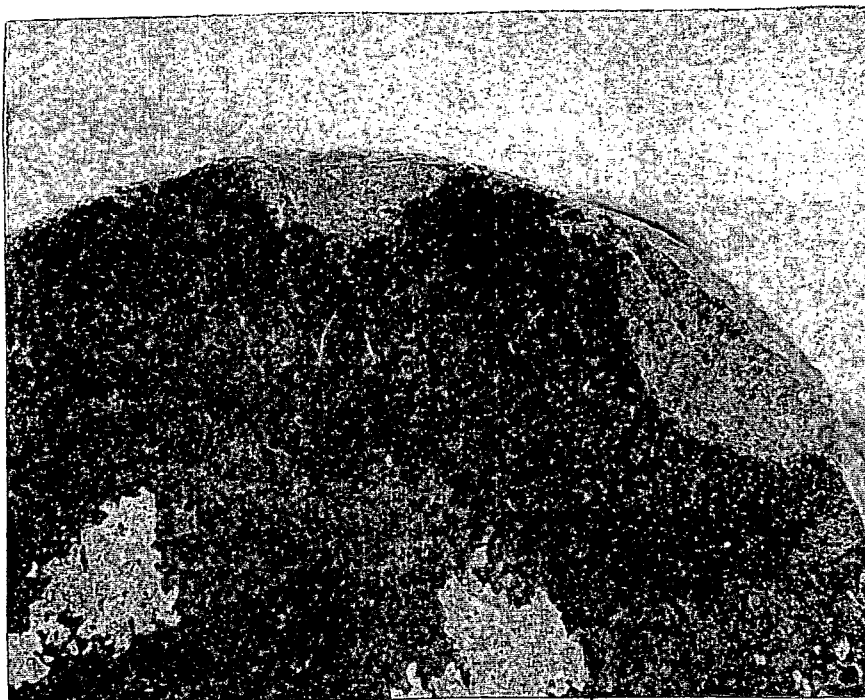


FIGURE 40. Close-up view of a fatigue crack initiation site on long dowel pin DL2. The surface pitting resulted from the chemical cleaning process. 10x

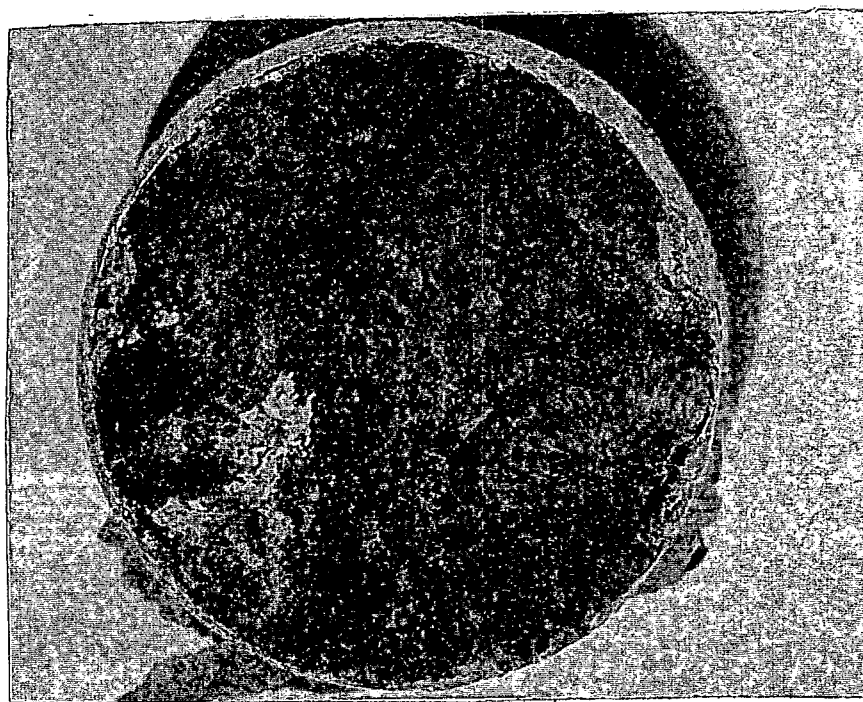


FIGURE 41. Appearance of the fracture face of long dowel pin DL2 after cleaning illustrating fatigue beach marks in the upper left side of the photo. 5x

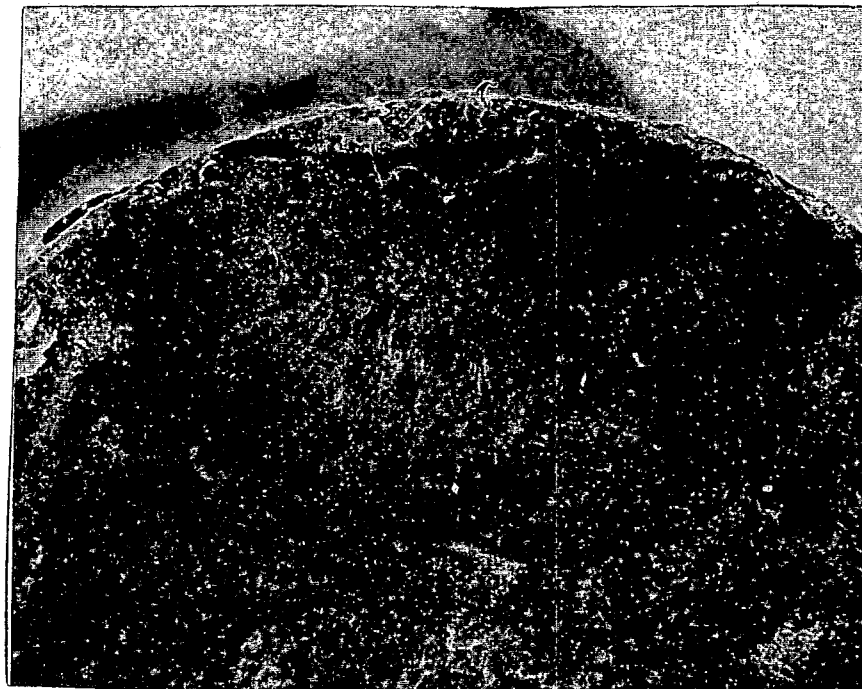


FIGURE 42. Close-up photo of the fatigue fracture origin on long dowel pin DL2. 10x

TABLE 1. 1989 As Found Condition of the Support Block Fasteners

	0°	60°	120°	180°	240°	300°
Bolt F4						
G6	Broken				Broken	
F8					Broken	
A3						
A9						
Pin B4						
Pin B8						
A5						
A7						

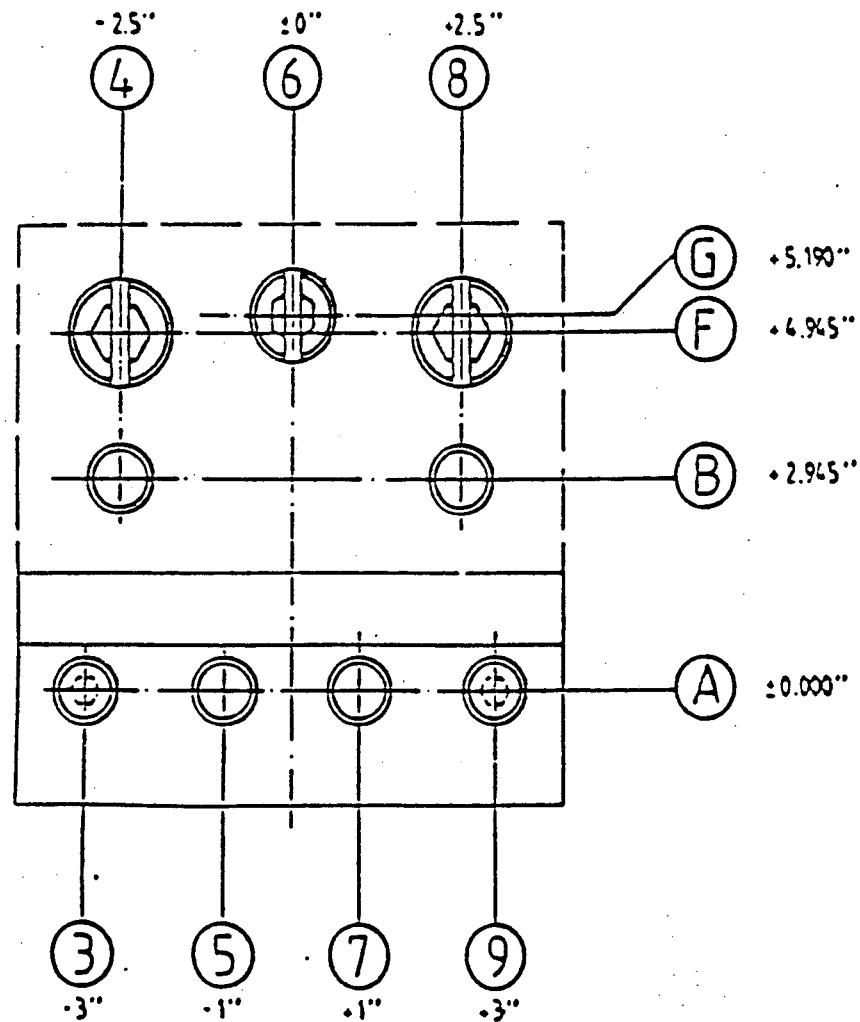


TABLE 2. 1990 As Found Condition of the Support Block Fasteners

	0°	60°	120°	180°	240°	300°
Bolt F4	Broken	Galled?	Broken		Broken	Broken
G6 Hidden BOLT	Broken	Broken Head/Bolt		Broken	Broken	Broken
F8	Broken	Galled?			Broken	
A3					Broken	
A9	Broken				Broken	
Pin B4	Loose				Loose	Loose
Pin B8	Loose					Loose
A5						
A7						

